

See discussions, stats, and author profiles for this publication at: <https://www.researchgate.net/publication/231374699>

# Experimental and Modeling Studies on High-Temperature Capture of CO<sub>2</sub> Using Lithium Zirconate Based Sorbents

ARTICLE *in* INDUSTRIAL & ENGINEERING CHEMISTRY RESEARCH · AUGUST 2007

Impact Factor: 2.59 · DOI: 10.1021/ie0616949

CITATIONS

42

READS

28

## 4 AUTHORS, INCLUDING:



**Gabriele Pannocchia**

Università di Pisa

85 PUBLICATIONS 940 CITATIONS

SEE PROFILE



**Monica Puccini**

Università di Pisa

39 PUBLICATIONS 220 CITATIONS

SEE PROFILE



**Sandra Vitolo**

Università di Pisa

63 PUBLICATIONS 1,177 CITATIONS

SEE PROFILE

# Experimental and Modeling Studies on High-Temperature Capture of CO<sub>2</sub> Using Lithium Zirconate Based Sorbents

Gabriele Pannocchia,\* Monica Puccini, Maurizia Seggiani, and Sandra Vitolo

Department of Chemical Engineering, Industrial Chemistry and Science of Materials, University of Pisa, Via Diotisalvi, 2, 56126 Pisa, Italy

Lithium zirconate (Li<sub>2</sub>ZrO<sub>3</sub>) is one of the most promising materials for CO<sub>2</sub> separation from flue gas at high temperature. This material is known to be able to adsorb a large amount of CO<sub>2</sub> around 500–600 °C. It was also reported that the addition of lithium/potassium carbonate to Li<sub>2</sub>ZrO<sub>3</sub> increased the CO<sub>2</sub> sorption rate when compared to pure Li<sub>2</sub>ZrO<sub>3</sub>. In this study, we examine the CO<sub>2</sub> sorption mechanism on Li<sub>2</sub>ZrO<sub>3</sub> by analyzing phase and microstructure changes of Li<sub>2</sub>ZrO<sub>3</sub> during the CO<sub>2</sub> sorption process with the help of thermogravimetric analysis, scanning electron microscopy, and X-ray diffraction analyses. We report on CO<sub>2</sub> sorption experiments for different Li<sub>2</sub>ZrO<sub>3</sub> based sorbents at different operating conditions in order to identify the most appropriate sorbent and experimental conditions. We also propose a kinetic model that is a variant of a double-shell model proposed in the literature by introducing additional dynamics to obtain a consistent response of the CO<sub>2</sub> uptake curve during the initial part of the sorption process. The proposed model, which has two temperature-dependent parameters that can be adjusted by regression on experimental data, shows excellent capabilities for describing the CO<sub>2</sub> uptake on a Li<sub>2</sub>ZrO<sub>3</sub> based sorbent.

## 1. Introduction

Carbon dioxide (CO<sub>2</sub>) is a greenhouse gas that is customarily released to the environment during the use of fossil fuels, including electric power generation. With the projected increase in consumption and demand for fossil fuels, CO<sub>2</sub> emissions will correspondingly increase in the absence of any capture/sequestration strategy. Given that CO<sub>2</sub> is a greenhouse gas with the potential to contribute to global climate warming, existing and improved technologies to mitigate the release of CO<sub>2</sub> to the environment are being considered as a prudent precaution against global warming. Therefore, the removal and recovery of carbon dioxide from power plant fuel gases is considered to be one of the effective approaches for reducing CO<sub>2</sub> emissions.

A number of techniques can be used for the separation of carbon dioxide from fuel gas streams. Physical absorption using amine solution is the only technology that is currently deployed commercially for CO<sub>2</sub> capture. However, there is a significant energy penalty associated with this technology, which operates at low temperature.

Recently, selective adsorption technology (using membrane or solid sorbents) has been identified as one of the ways to capture CO<sub>2</sub> at high temperature, without cooling the flue gas to ambient or even lower temperature. For the separation of carbon dioxide from hot gas stream, the adsorbent must have high selectivity for CO<sub>2</sub> over N<sub>2</sub> at elevated temperatures and high adsorption capacity for carbon dioxide at the operating temperature.

The development of inorganic membranes for CO<sub>2</sub> separation, such as zeolite, sol–gel derived zirconia, and sol–gel derived silica membranes, has received increasing attention in the past few years.<sup>1</sup> However, these inorganic membranes do not offer sufficiently high permselectivity for separation of CO<sub>2</sub> over N<sub>2</sub> at temperatures greater than 350 °C.<sup>2</sup>

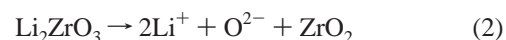
Among the various solid sorbents that have been studied, carbon-based adsorbents, metal oxide sorbents,<sup>3</sup> and hydrotal-

cite-like compounds<sup>4,5</sup> can be used as adsorbents for the removal of carbon dioxide from hot flue gas. However, the sorption capacity of these materials is low and the adsorption capacity of CO<sub>2</sub> decreases during adsorption/desorption cycles.<sup>6,7</sup>

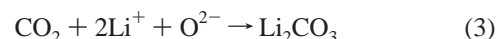
Lithium zirconate (Li<sub>2</sub>ZrO<sub>3</sub>) is another material for CO<sub>2</sub> separation from flue gas at high temperature that has received increasing attention in the past few years. This material is known to be able to adsorb a large amount of CO<sub>2</sub> around 500–600 °C. The main advantages of this material are its lower regeneration temperature (750 °C) compared to current mineral origin based sorbents, which tend to sinter at high temperatures, and its stability that allows operation over a significant number of cycles without losing its sorption capacity. Li<sub>2</sub>ZrO<sub>3</sub> can adsorb CO<sub>2</sub> through its sorption mechanism based on the following reaction:



From a kinetic point of view, the reaction occurs in two steps. First, Li<sub>2</sub>ZrO<sub>3</sub> decomposes according to the following reaction:



Then, CO<sub>2</sub> reacts with lithium and oxygen ions to produce Li<sub>2</sub>CO<sub>3</sub>:



Lithium zirconate does not react with N<sub>2</sub> at all; thus, it could give an infinitely large CO<sub>2</sub>/N<sub>2</sub> selectivity.

A double-shell model to describe the sorption mechanism of CO<sub>2</sub> on Li<sub>2</sub>ZrO<sub>3</sub> was proposed by Ida and Lin.<sup>2</sup> According to this model, which is schematically shown in Figure 1, the CO<sub>2</sub> sorption mechanism can be described as follows. During the sorption process carbon dioxide diffuses to the surface of Li<sub>2</sub>ZrO<sub>3</sub> and reacts with Li<sup>+</sup> and O<sup>2-</sup> on the surface to form ZrO<sub>2</sub> and Li<sub>2</sub>CO<sub>3</sub>. Zirconium oxide forms a solid shell that covers unreacted Li<sub>2</sub>ZrO<sub>3</sub>, and similarly, Li<sub>2</sub>CO<sub>3</sub> forms another shell outside the ZrO<sub>2</sub> shell. Therefore, during the carbonation process the sorption rate begins to decrease because Li<sup>+</sup> and O<sup>2-</sup>

\* To whom correspondence should be addressed. Tel.: +39 050 511238. Fax: +39 050 511266. E-mail: g.pannocchia@ing.unipi.it.

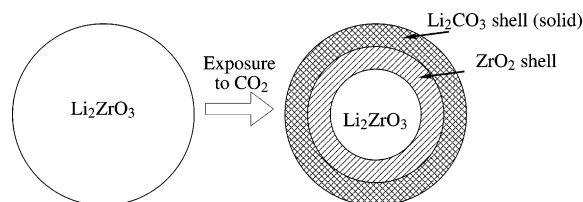


**Figure 1.** Schematic illustration of double-shell model for  $\text{CO}_2$  sorption on  $\text{Li}_2\text{ZrO}_3$ .

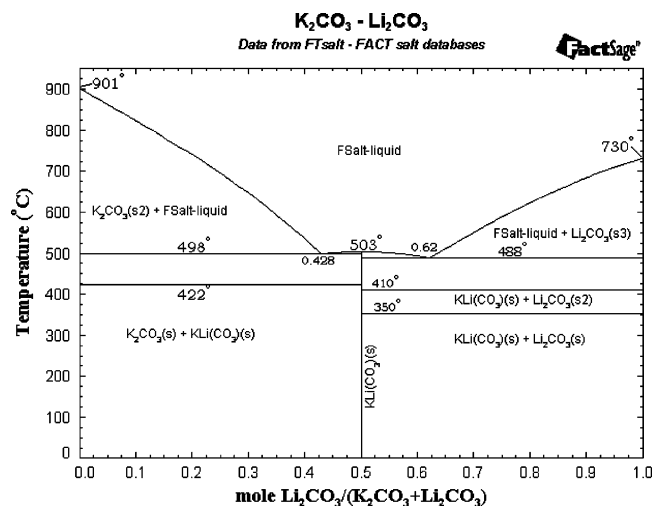


**Figure 2.** Phase diagram of  $\text{Li}_2\text{CO}_3/\text{K}_2\text{CO}_3$ .

have to diffuse through this  $\text{ZrO}_2$  shell to react with  $\text{CO}_2$  and carbon dioxide molecules have to diffuse through the  $\text{Li}_2\text{CO}_3$  shell for reaction. It was found that pure  $\text{Li}_2\text{ZrO}_3$  has a very slow  $\text{CO}_2$  sorption rate. However, doping  $\text{Li}_2\text{CO}_3/\text{K}_2\text{CO}_3$  into  $\text{Li}_2\text{ZrO}_3$  can substantially increase the sorption rate because  $\text{Li}_2\text{CO}_3/\text{K}_2\text{CO}_3$  dopant can form eutectic molten carbonate at high temperature (e.g.,  $500^\circ\text{C}$ ). This molten carbonate “shell” can greatly reduce  $\text{CO}_2$  diffusion resistance compared to the solid  $\text{Li}_2\text{CO}_3$  shell in the pure  $\text{Li}_2\text{ZrO}_3$  case. Moreover, the oxygen ion diffusion through the  $\text{ZrO}_2$  shell can be improved by doping lithium zirconate with yttrium oxide,  $\text{Y}_2\text{O}_3$ .<sup>8,9</sup>

In this study, we synthesized several lithium zirconate based sorbents, pure and modified with carbonates and/or yttrium, and we characterized them using scanning electron microscopy (SEM) and X-ray diffraction (XRD) analyses. We also conducted  $\text{CO}_2$  sorption experiments at different operating conditions with the help of thermogravimetric analysis (TGA). Furthermore, in this paper we describe the sorption process of  $\text{CO}_2$  on a proposed  $\text{Li}_2\text{ZrO}_3$  based sorbent with a mathematical model that is similar to the double-shell model present in the literature,<sup>2,6,8</sup> but contains a number of modifications to make it more adherent to some theoretical and experimental observations.

## 2. Experimental Materials and Methods

**2.1. Sorbent Preparation.** Pure  $\text{Li}_2\text{ZrO}_3$  powders were prepared by the solid-state method. Starting materials were reagent-grade  $\text{Li}_2\text{CO}_3$  and  $\text{ZrO}_2$  (from Aldrich) in a 1:1 molar ratio. The materials were weighed, mixed, and ground in an agate mortar with a suitable amount of acetone. Then, the mixtures were dried and calcined in air at  $850^\circ\text{C}$  for 6 h. Both temperature increase and decrease ramping rates were set to  $60^\circ\text{C}/\text{h}$ . After calcination the products were ground to powder again in the agate mortar for later analysis.

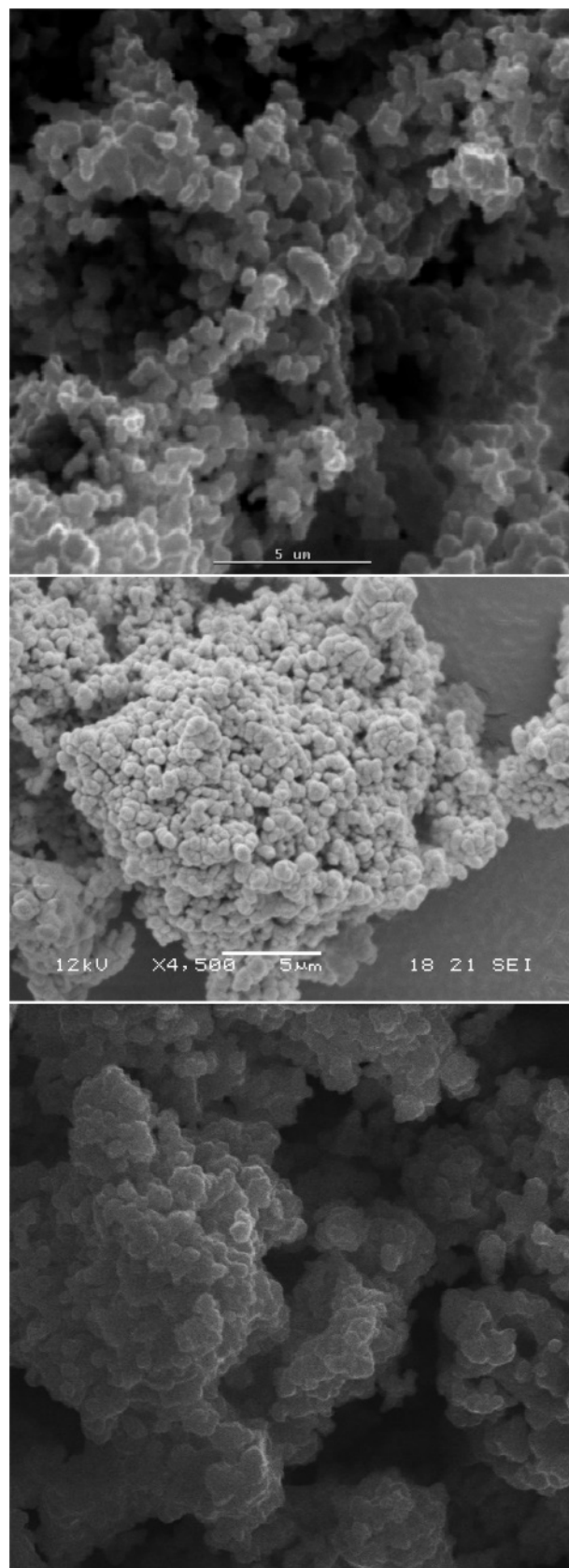


**Figure 3.** SEM images of pure (top),  $\text{Li}_2\text{CO}_3/\text{K}_2\text{CO}_3$ -doped  $\text{Li}_2\text{ZrO}_3$  (middle), and  $\text{Li}_2\text{ZrO}_3$  prepared with addition of  $\text{Y}_2\text{O}_3$  (bottom).

Powders of  $\text{Li}_2\text{ZrO}_3$  with  $\text{K}_2\text{CO}_3$  (from Aldrich) were also prepared using the same preparation procedure mentioned above. Two different compositions of sorbents were tested. It is known that the mixture of  $\text{Li}_2\text{CO}_3$  and  $\text{K}_2\text{CO}_3$  can form a eutectic

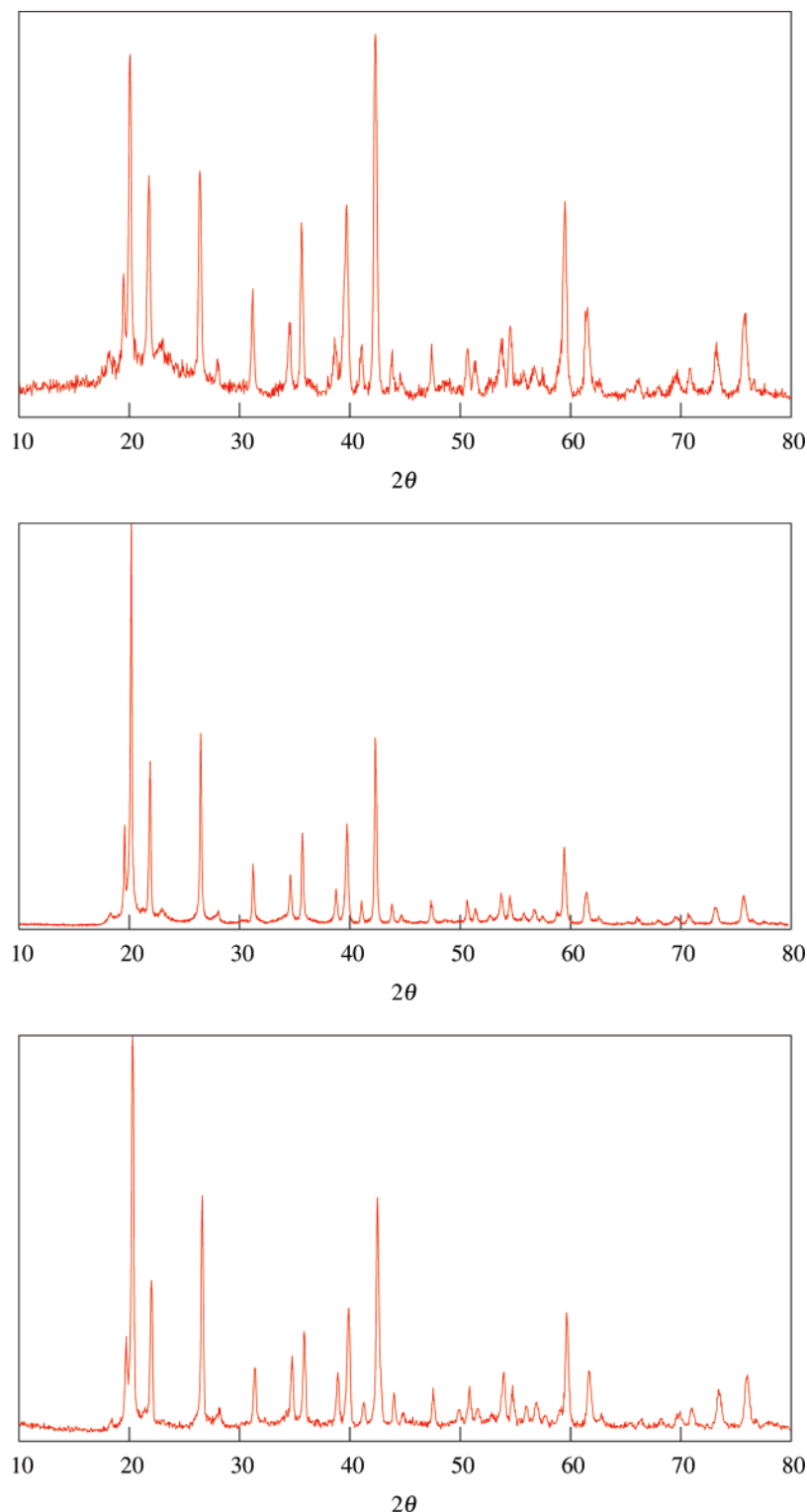


**Figure 4.** XRD patterns of pure  $\text{Li}_2\text{ZrO}_3$  (top),  $\text{Li}_2\text{CO}_3/\text{K}_2\text{CO}_3$ -doped  $\text{Li}_2\text{ZrO}_3$  with 10% excess  $\text{Li}_2\text{CO}_3$  (middle), and  $\text{Li}_2\text{CO}_3/\text{K}_2\text{CO}_3$ -doped  $\text{Li}_2\text{ZrO}_3$  with 15% excess  $\text{Li}_2\text{CO}_3$  (bottom).

mixture having melting point of 498 °C, as shown in Figure 2. At the sorption temperature (e.g., 550 °C) the mixture of Li and K carbonates is partially or totally liquid depending on their composition ratio in the mixture. Thus, the molar ratios of the starting materials ( $\text{Li}_2\text{CO}_3:\text{ZrO}_2:\text{K}_2\text{CO}_3$ ) considered in this work were 1.1:1.0:0.2 (typical composition suggested in the literature<sup>6,8</sup>) and 1.15:1.0:0.2, in order to have a completely molten carbonate at the start of the sorption reaction. For the typical

potassium-doped lithium zirconate, the reaction of calcination can be represented as follows:



in which one can notice that a 10% excess of  $\text{Li}_2\text{CO}_3$  is used. Using this excess of  $\text{Li}_2\text{CO}_3$ , a 0.33  $\text{Li}_2\text{CO}_3$  mole fraction in

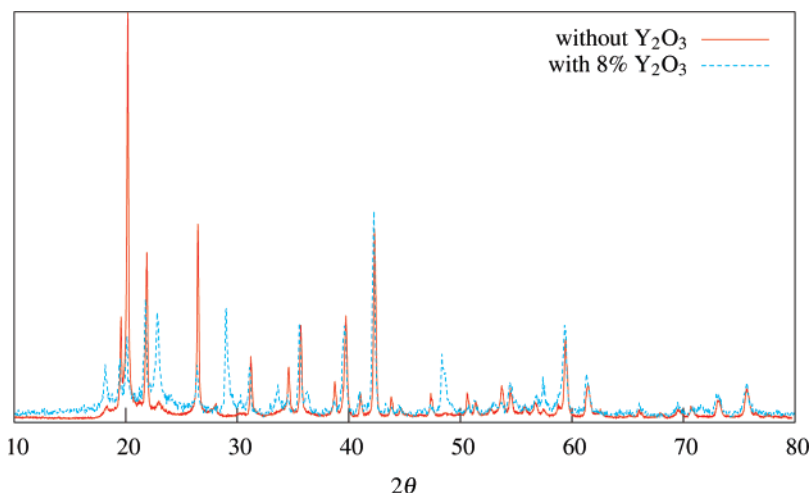


Figure 5. XRD patterns of  $\text{Li}_2\text{CO}_3/\text{K}_2\text{CO}_3$ -doped  $\text{Li}_2\text{ZrO}_3$  with 10% excess  $\text{Li}_2\text{CO}_3$  prepared from pure  $\text{ZrO}_2$  and with addition of 8%  $\text{Y}_2\text{O}_3$ .

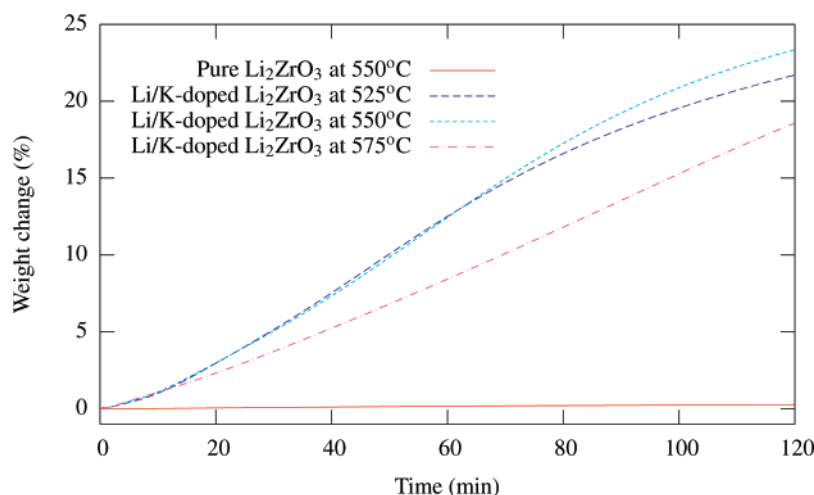


Figure 6.  $\text{CO}_2$  uptake of pure and  $\text{Li}_2\text{CO}_3/\text{K}_2\text{CO}_3$ -doped  $\text{Li}_2\text{ZrO}_3$  with 10% excess  $\text{Li}_2\text{CO}_3$  at different temperatures.

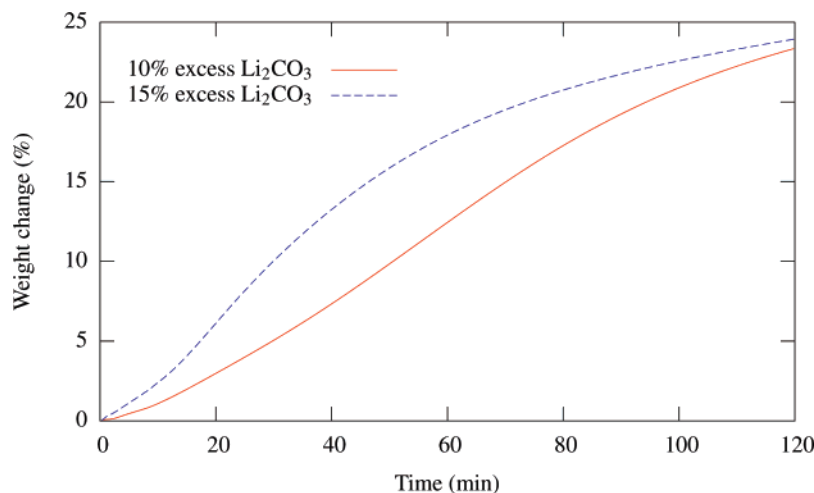
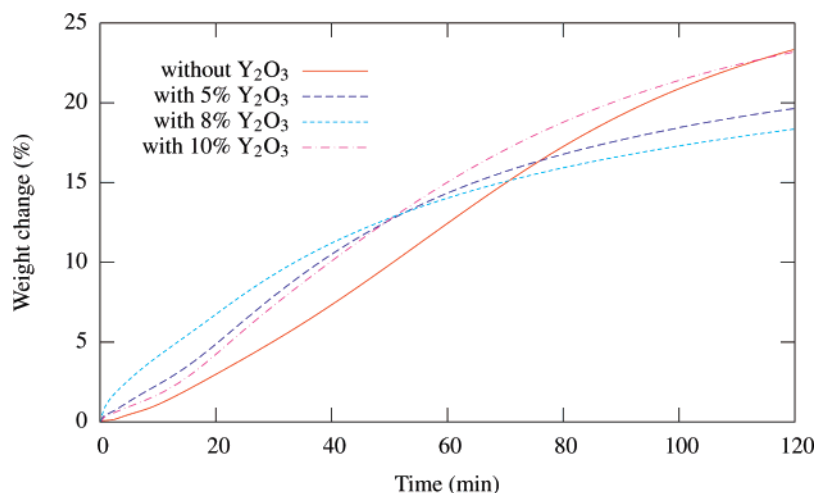


Figure 7.  $\text{CO}_2$  uptake on  $\text{Li}_2\text{CO}_3/\text{K}_2\text{CO}_3$ -doped  $\text{Li}_2\text{ZrO}_3$  with different excess amounts of  $\text{Li}_2\text{CO}_3$  (at 550 °C).

the carbonate mixture is achieved, and from Figure 2 we can see that, at the operating temperature (between 500 and 600 °C, as discussed later on), a solid phase is also present along with the eutectic liquid phase. For the sorbent prepared with a 15% excess of  $\text{Li}_2\text{CO}_3$ , instead, a 0.43  $\text{Li}_2\text{CO}_3$  mole fraction in the carbonate mixture is achieved, and from Figure 2 we can see that only a liquid phase is present at the operating temperature.

The samples with  $\text{K}_2\text{CO}_3$  and  $\text{Y}_2\text{O}_3$  (from Aldrich), for producing yttrium-doped lithium zirconate, were prepared by the solid-state method suggested by Zou and Petric,<sup>10</sup> as described above.  $\text{Y}_2\text{O}_3$  was used in order to improve the  $\text{O}^{2-}$  ion diffusion rate in the  $\text{ZrO}_2$  shell. It is well-known that oxygen ions diffuse through  $\text{ZrO}_2$  via oxygen vacancies in  $\text{ZrO}_2$  crystals. Pure  $\text{ZrO}_2$  has a monoclinic structure at room temperature. When doped with yttrium oxide,  $\text{ZrO}_2$  is



**Figure 8.**  $\text{CO}_2$  uptake of  $\text{Li}_2\text{CO}_3/\text{K}_2\text{CO}_3$ -doped  $\text{Li}_2\text{ZrO}_3$  with 10% excess  $\text{Li}_2\text{CO}_3$  prepared from pure  $\text{ZrO}_2$  and with addition of  $\text{Y}_2\text{O}_3$  at different molar ratios (at 550 °C).

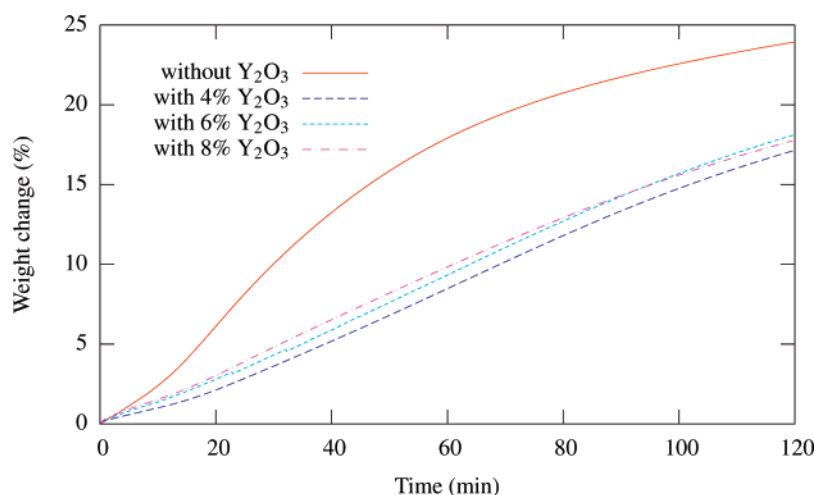


**Figure 9.**  $\text{CO}_2$  uptake of  $\text{Li}_2\text{CO}_3/\text{K}_2\text{CO}_3$ -doped  $\text{Li}_2\text{ZrO}_3$  with 15% excess  $\text{Li}_2\text{CO}_3$  prepared from pure  $\text{ZrO}_2$  and with addition of  $\text{Y}_2\text{O}_3$  at different molar ratios (at 550 °C).

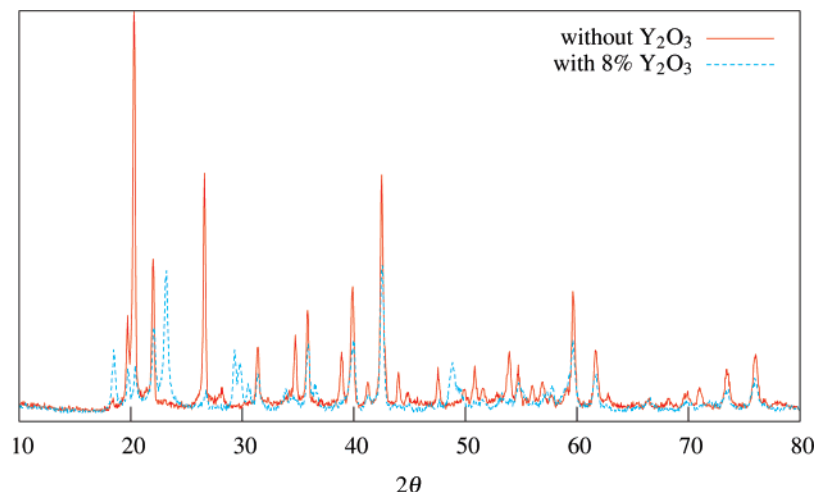


**Figure 10.** XRD patterns of  $\text{Li}_2\text{CO}_3/\text{K}_2\text{CO}_3$ -doped  $\text{Li}_2\text{ZrO}_3$  with 15% excess  $\text{Li}_2\text{CO}_3$  prepared from pure  $\text{ZrO}_2$  and with addition of 8%  $\text{Y}_2\text{O}_3$ .

fully stabilized. The replacement of  $\text{Zr}^{4+}$  by  $\text{Y}^{3+}$  give rise to a higher concentration of structural oxygen vacancies for charge compensation and stabilizes the cubic phase. At high temperatures, these oxygen vacancies are highly mobile and give rise to oxygen ionic conductivity via a vacancy diffusion mechanism. The highest ionic conductivities were reported for  $\text{Y}_2\text{O}_3$  concentrations of 7–10%.<sup>11</sup> In particular, in

this work for sorbents prepared with a 10% excess of  $\text{Li}_2\text{CO}_3$ , lithium zirconate was doped with 5, 8, and 10%  $\text{Y}_2\text{O}_3$ , whereas for sorbents prepared with a 15% excess of  $\text{Li}_2\text{CO}_3$ , lithium zirconate was doped with 4, 6, and 8%  $\text{Y}_2\text{O}_3$ .

**2.2. Experimental Procedures.** Carbon dioxide sorption on prepared powders was studied using a TGA Q500 (from TA Instrument). About 20 mg sample was placed in the sample



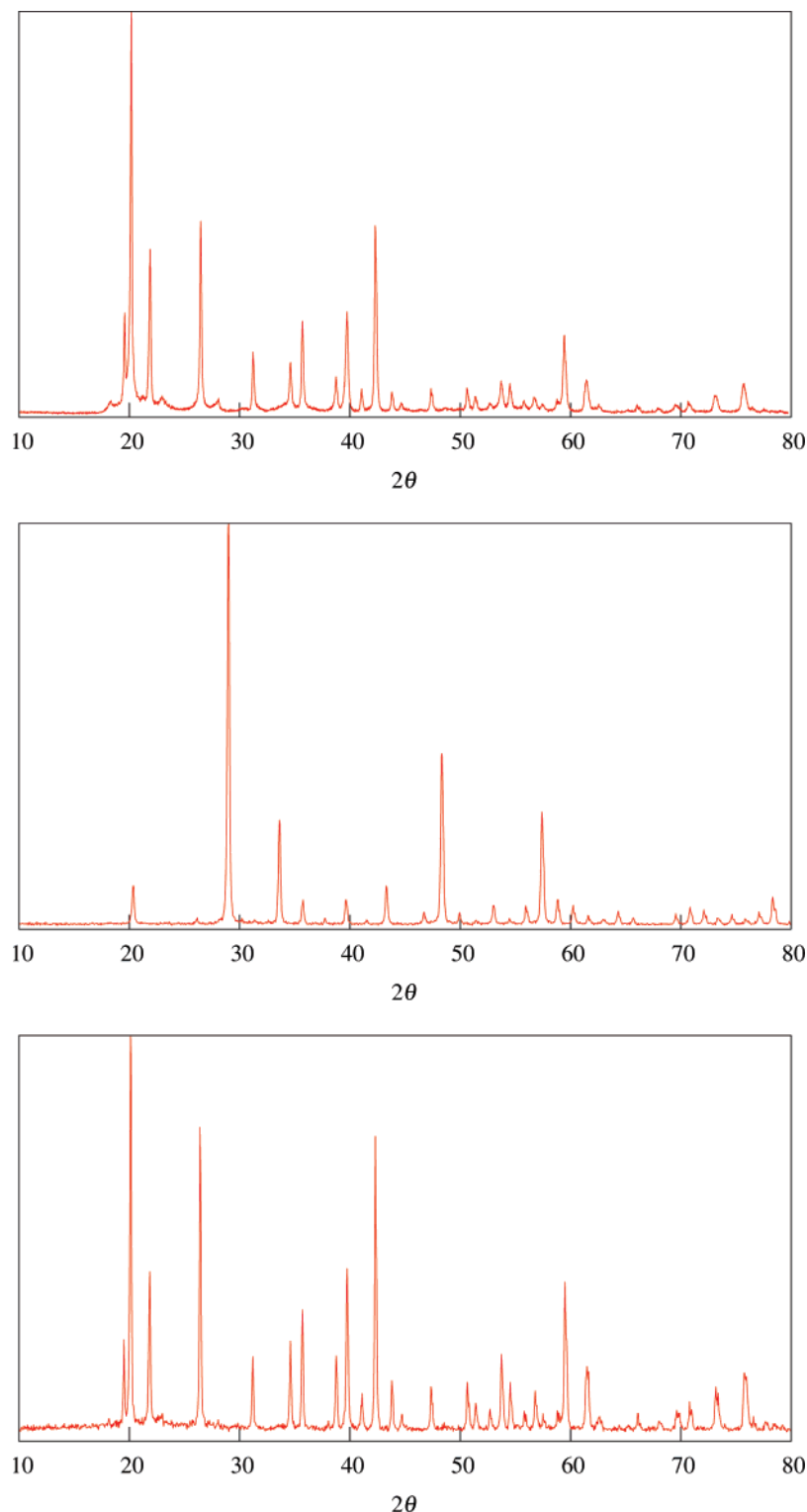


**Figure 11.** XRD patterns of  $\text{Li}_2\text{CO}_3/\text{K}_2\text{CO}_3$ -doped  $\text{Li}_2\text{ZrO}_3$  before (top) and during (middle)  $\text{CO}_2$  sorption and after  $\text{CO}_2$  desorption (bottom).

pan, and before adsorbing carbon dioxide the sample was dried at the operating temperature by passing nitrogen flow until the sample weight became stable.  $\text{CO}_2$  partial pressures were set up by controlling the composition of the feed ( $\text{CO}_2/\text{N}_2$ ) using mass flow controllers. The total feed gas flow rate was maintained at 100 mL/min (60%  $\text{CO}_2$ , 40%  $\text{N}_2$ ). The sample was heated to the desired temperature with a ramp rate of 10 °C/min and the measurement of the sample weight gain versus time after the inlet flow was changed from  $\text{N}_2$  to the premixed  $\text{CO}_2/\text{N}_2$  mixture was recorded. After that,  $\text{CO}_2$  desorption was performed by raising the temperature to 800 °C with ramp rate

of 10 °C/min and changing from  $\text{CO}_2/\text{N}_2$  mixture to nitrogen. A tubular furnace was used to control the temperature, and  $\text{CO}_2$  sorption was conducted at different temperatures in order to study the temperature effect on the sorption rate.

The phase structure of the prepared samples was examined by powder X-ray diffraction analysis (XRD) using a Siemens D 500 XRD with  $\text{Cu K}\alpha$  radiation. The XRD patterns were recorded over a  $2\theta$  range of 10°–80°. Phase identification was verified by comparison against the powder diffraction patterns reported in ref 8. The morphology of the obtained powders was observed using a JEOL 5600LV scanning electron microscope

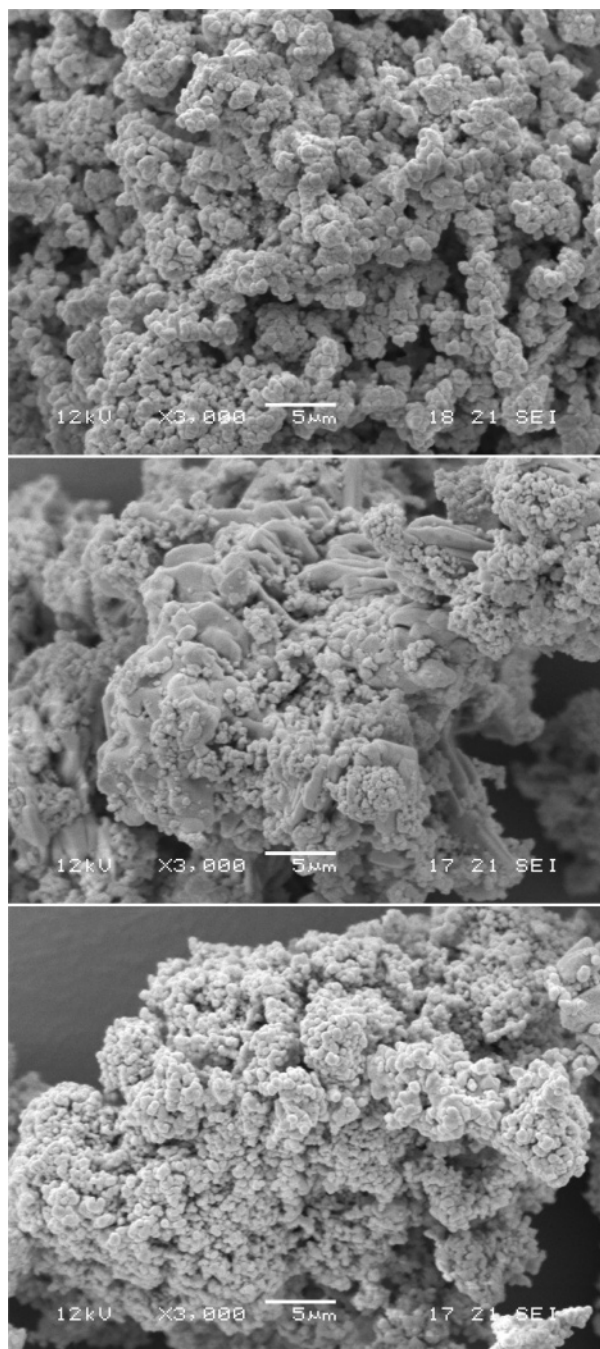


**Figure 12.** SEM images of  $\text{Li}_2\text{CO}_3/\text{K}_2\text{CO}_3$ -doped  $\text{Li}_2\text{ZrO}_3$  before (top) and during (middle)  $\text{CO}_2$  sorption and after  $\text{CO}_2$  desorption (bottom).

(SEM). XRD and SEM analyses were also used to evaluate the structural changes of the sorbent during a  $\text{CO}_2$  sorption/desorption cycle. In particular, in order to characterize the sorption products, the sorbent was rapidly quenched to room temperature after  $\text{CO}_2$  sorption at  $550^\circ\text{C}$ , and the obtained powder was analyzed. Similarly, the sorbent was characterized after  $\text{CO}_2$  desorption at  $800^\circ\text{C}$ .

### 3. Experimental Results and Discussion

**3.1. Sorbent Characterization.** Microscopic views of the pure  $\text{Li}_2\text{ZrO}_3$ ,  $\text{Li}_2\text{CO}_3/\text{K}_2\text{CO}_3$ -doped  $\text{Li}_2\text{ZrO}_3$ , and lithium zirconate prepared with addition of 8%  $\text{Y}_2\text{O}_3$  are presented in Figure 3. Particles have relatively uniform size and they stick together to form a large porous agglomerate. Moreover, the average particle size is around  $1\ \mu\text{m}$ : the particle size of  $\text{Li}_2\text{ZrO}_3$

was controlled by  $\text{ZrO}_2$  because during the preparation (calcination) only  $\text{ZrO}_2$  particles remained in the solid state due to its high melting point ( $2700^\circ\text{C}$ ). Therefore,  $\text{ZrO}_2$  particles acted as cores to control the particle size of product  $\text{Li}_2\text{ZrO}_3$ .<sup>6</sup> In this work,  $\text{ZrO}_2$  powder of particle size below  $1\ \mu\text{m}$  was used. In the case of  $\text{Li}_2\text{CO}_3/\text{K}_2\text{CO}_3$ -doped  $\text{Li}_2\text{ZrO}_3$ , the mixture of lithium and potassium carbonates are also in the liquid state during the preparation process because the melting point of their mixture is much lower than the preparation temperature. In this case, an excess amount of lithium/potassium carbonates may remain on the surface of the  $\text{Li}_2\text{ZrO}_3$  after the  $\text{Li}_2\text{ZrO}_3$  formation reaction is completed.

The X-ray diffraction patterns of the prepared  $\text{Li}_2\text{ZrO}_3$  powders, pure and modified with carbonates, are presented in Figure 4. As can be seen, the prepared pure lithium zirconate presents most diffraction peaks assigned to  $\text{Li}_2\text{ZrO}_3$  monoclinic.<sup>8</sup> Patterns of the  $\text{Li}_2\text{CO}_3/\text{K}_2\text{CO}_3$ -doped  $\text{Li}_2\text{ZrO}_3$  sample also present characteristic peaks of pure lithium zirconate, independently of the  $\text{Li}_2\text{CO}_3$  excess.

Figure 5 shows XRD patterns of Li/K-doped  $\text{Li}_2\text{ZrO}_3$  with a 10% excess of  $\text{Li}_2\text{CO}_3$  prepared from pure  $\text{ZrO}_2$  and with the addition of 8%  $\text{Y}_2\text{O}_3$ . As can be seen, the diffraction peaks for the sample prepared with the addition of  $\text{Y}_2\text{O}_3$  can be matched with those of  $\text{Li}_2\text{ZrO}_3$  except for two small peaks, which may be assigned to zirconia. The XRD results also show that the diffraction peaks systematically shift toward lower diffraction angles. Since the geometry of the crystal structure is correlated to the angular position of the diffraction peaks (according to Bragg's law), the observed shift suggests an increase of the distance between crystallographic planes due to the presence of  $\text{Y}_2\text{O}_3$  in the crystal structure of zirconia. Hence, these results indicate that we obtained a solid solution of  $\text{Y}_2\text{O}_3$ -doped  $\text{Li}_2\text{ZrO}_3$ .<sup>10</sup>

**3.2. Sorption Properties.** The  $\text{CO}_2$  uptake curve on the pure lithium zirconate sorbent is reported in Figure 6. As can be seen, the sorption rate is very low (the weight change after 40 min was only 0.10%). Figure 6 also shows sorption curves, at different temperatures ( $525$ ,  $550$ , and  $575^\circ\text{C}$ ), on  $\text{Li}_2\text{ZrO}_3$  with carbonates having a molar ratio  $\text{Li}_2\text{CO}_3:\text{K}_2\text{CO}_3:\text{ZrO}_2$  equal to 1.1:1.0:0.2. As shown, the sorption rate on modified  $\text{Li}_2\text{ZrO}_3$  is much higher than that on pure lithium zirconate. This higher sorption rate on Li/K-doped  $\text{Li}_2\text{ZrO}_3$  can be explained by the formation of a liquid phase of potassium lithium carbonate (which is molten at temperatures above  $500^\circ\text{C}$ ) between sorbent particles during the carbonation reaction. Diffusion of  $\text{CO}_2$  in the molten carbonate is several orders of magnitude higher than that in the solid carbonate, which instead forms in the case of pure  $\text{Li}_2\text{ZrO}_3$ . Then, for Li/K-doped lithium zirconate the rate-limiting step is now switched to diffusion of  $\text{Li}^+$  and  $\text{O}^{2-}$  through the zirconium oxide shell which forms surrounding the unreacted lithium zirconate core during the sorption reaction. From Figure 6 we can also see that the sorption rate increases as the temperature increases from  $525$  to  $550^\circ\text{C}$ . However, when the temperature continues to increase from  $550$  to  $575^\circ\text{C}$ , the sorption rate decreases. This suggests that temperature affects the sorption rate in two opposite directions. Increasing the temperature can increase the reaction rate constant. However, increasing the temperature would increase the equilibrium carbon dioxide partial pressure and thus reduce the driving force for sorption at the constant operation  $\text{CO}_2$  pressure. The temperature effect on the sorption rate depends on both thermo-



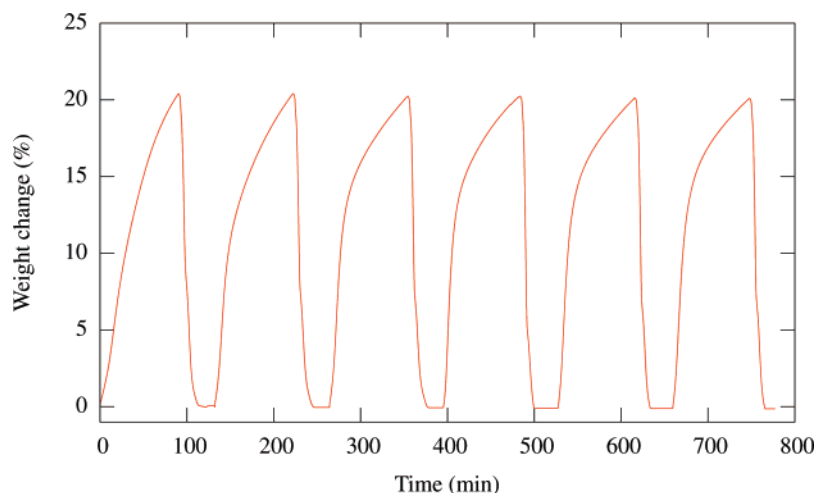


**Figure 13.** CO<sub>2</sub> uptake and release of Li<sub>2</sub>CO<sub>3</sub>/K<sub>2</sub>CO<sub>3</sub>-doped Li<sub>2</sub>ZrO<sub>3</sub> with 15% excess Li<sub>2</sub>CO<sub>3</sub> during six cycles of sorption at 550 °C and desorption at 800 °C.

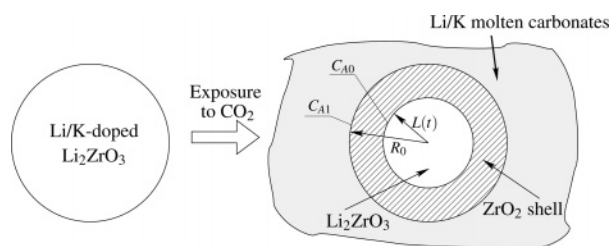


**Figure 14.** Schematic illustration of kinetic model for CO<sub>2</sub> sorption on Li<sub>2</sub>CO<sub>3</sub>/K<sub>2</sub>CO<sub>3</sub>-doped Li<sub>2</sub>ZrO<sub>3</sub>.

dynamic and kinetic factors. A moderate temperature range, e.g., around 550 °C, would be desirable for carbon dioxide sorption.

CO<sub>2</sub> uptake curves on lithium zirconate with different proportions between carbonates in the starting mixture are reported in Figure 7. As can be seen, during the first 120 min of operation, the sorption rate on a sorbent prepared with a 15% excess of Li<sub>2</sub>CO<sub>3</sub> is higher than that of a sorbent prepared with a 10% excess of Li<sub>2</sub>CO<sub>3</sub>. This higher sorption rate depends on the different condition of the Li<sub>2</sub>CO<sub>3</sub>/K<sub>2</sub>CO<sub>3</sub> mixture at the sorption temperature (550 °C) at the start of the carbonation (Figure 2): in the case of a 15% excess of Li<sub>2</sub>CO<sub>3</sub> the mixture is completely molten; thus the CO<sub>2</sub> diffusion is enhanced in the liquid phase.

In order to improve the O<sup>2-</sup> ion diffusion rate in the ZrO<sub>2</sub> shell, lithium zirconate with carbonate was prepared with addition of Y<sub>2</sub>O<sub>3</sub>. Figures 8 and 9 show CO<sub>2</sub> uptake curves on these sorbents. The operation temperature is 550 °C. In the case of sorbents with composition Li<sub>2</sub>CO<sub>3</sub>:ZrO<sub>2</sub>:K<sub>2</sub>CO<sub>3</sub> = 1.1:1.0:0.2, the sorbent with yttria gives a higher CO<sub>2</sub> sorption rate, during the first 60 min of operation, than the sample without yttria in accordance with the increase of oxygen vacancies due the introduction of Y<sub>2</sub>O<sub>3</sub> into ZrO<sub>2</sub>. Moreover, during the first part of the sorption process, the sorption rate decreases for Y<sub>2</sub>O<sub>3</sub> concentration higher than 8%. Although an increasing number of vacancies is obtained when the dopant concentration is raised, the vacancy mobility decreases, and at sufficiently high concentrations, the latter factor starts to dominate leading to a decrease of conductivity.<sup>12</sup> In particular, 8% Y<sub>2</sub>O<sub>3</sub> substitution for ZrO<sub>2</sub> leads to a composition close to the lower limit for stabilization of the zirconium oxide with the highest value of electrical conductivity.<sup>13</sup> The samples having composition Li<sub>2</sub>CO<sub>3</sub>:ZrO<sub>2</sub>:K<sub>2</sub>CO<sub>3</sub> = 1.15:1.0:0.2 do not present the same trend. This difference can be explained by the XRD patterns of the

sorbents. Figure 10 reports results of X-ray analysis of this sorbent without yttria and with 8% Y<sub>2</sub>O<sub>3</sub>. As can be seen, the shift of diffraction peaks toward lower diffraction angles is absent. This suggests that the presence of a larger excess of carbonates may prevent Y<sub>2</sub>O<sub>3</sub> from doping the crystal structure to increase oxygen vacancies.

To summarize, based on the experimental results presented in this section, as well as other ones not shown for the sake of space, we believe that the most promising sorbent among those compared in this study is that having composition Li<sub>2</sub>CO<sub>3</sub>:ZrO<sub>2</sub>:K<sub>2</sub>CO<sub>3</sub> = 1.15:1.0:0.2, without the necessity of adding such an expensive component as yttrium.

**3.3. Sorbent Characterization during Sorption/Desorption Cycles.** For the sorbent of choice, we conducted further studies in order to assess its regeneration properties and stability during several cycles of sorption and desorption. Figure 11 shows, by means of X-ray analysis, the microstructure changes of the Li/K-doped Li<sub>2</sub>ZrO<sub>3</sub> before and during CO<sub>2</sub> sorption and after CO<sub>2</sub> desorption. Compared to XRD patterns of the original sorbent (top of Figure 11), XRD patterns of the sorption product (middle of Figure 11) show that the peaks assigned to Li<sub>2</sub>ZrO<sub>3</sub> completely disappeared and that ZrO<sub>2</sub> peaks are present instead. This result indicates that during the CO<sub>2</sub> sorption process Li<sub>2</sub>ZrO<sub>3</sub> reacts with CO<sub>2</sub> to become ZrO<sub>2</sub> and Li<sub>2</sub>CO<sub>3</sub>. However, the peaks of Li<sub>2</sub>CO<sub>3</sub> were undetectable: Li<sub>2</sub>CO<sub>3</sub> produced by the carbonation reaction is in liquid state; thus the carbonate becomes amorphous and undetectable by XRD after it is quenched. XRD patterns of the regenerated sorbent (bottom of Figure 11) only show peaks assigned to monoclinic Li<sub>2</sub>ZrO<sub>3</sub>, without other peaks. This means that, after CO<sub>2</sub> desorption at 800 °C, Li<sub>2</sub>CO<sub>3</sub> and ZrO<sub>2</sub> react to produce again Li<sub>2</sub>ZrO<sub>3</sub> with a monoclinic structure by releasing CO<sub>2</sub>. Figure 12 shows SEM images of Li/K-doped Li<sub>2</sub>ZrO<sub>3</sub> before and during CO<sub>2</sub> sorption and after CO<sub>2</sub> desorption. By comparison of SEM images of the original sorbent (top of Figure 12) and of the sorption product (middle of Figure 12), we can notice in the latter SEM image the presence of an amorphous phase associated with the quenched liquid carbonates. Furthermore, the SEM image of the regenerated sorbent (bottom of Figure 12) is essentially “identical” to that of the original sorbent. Hence, the sorbent appears to be fully regenerable.

Finally, we tested the stability of the sorbent undergoing several cycles of CO<sub>2</sub> sorption and desorption. In particular, Figure 13 shows CO<sub>2</sub> uptake and release of the sorbent during six cycles of sorption and desorption. It can be seen that no

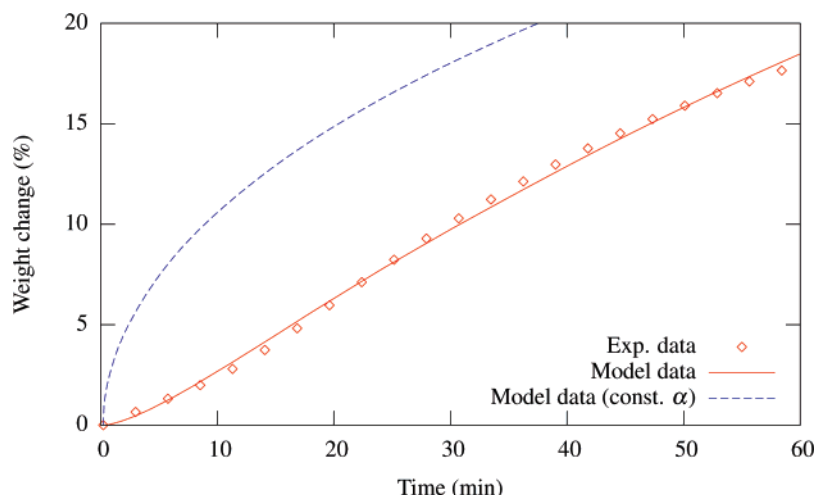


Figure 15. Experimental and model CO<sub>2</sub> uptake curves on Li<sub>2</sub>CO<sub>3</sub>/K<sub>2</sub>CO<sub>3</sub>-doped Li<sub>2</sub>ZrO<sub>3</sub> with 15% excess Li<sub>2</sub>CO<sub>3</sub> at 550 °C.

Table 1. Optimized Model Parameters at Different Temperatures

temp (°C)	500	550	600
$\tau$ (min)	14.6	14.3	15.0
$\bar{\alpha}$ (s <sup>-1</sup> )	$0.74 \times 10^{-6}$	$1.90 \times 10^{-6}$	$0.16 \times 10^{-6}$

differences are noticed in terms of sorption capacity among different cycles, and therefore the sorbent appears fully stable.

#### 4. Model Development

**4.1. Introduction.** Ida and Lin<sup>2</sup> proposed a double-shell model, schematically depicted in Figure 1, to describe the CO<sub>2</sub> sorption mechanism on Li<sub>2</sub>ZrO<sub>3</sub> from a qualitative point of view. A mathematical formulation based on this model was proposed by Ida et al.<sup>8</sup> for the case of CO<sub>2</sub> sorption on pure Li<sub>2</sub>ZrO<sub>3</sub>, and was appropriately modified by Xiong et al.<sup>6</sup> for the case of Li<sub>2</sub>-ZrO<sub>3</sub> sorbent modified with Li<sub>2</sub>CO<sub>3</sub>/K<sub>2</sub>CO<sub>3</sub> (it must be noticed that, despite the publication year, ref 8 was submitted slightly earlier than ref 6). The main difference between these two mathematical models is that in the case of pure Li<sub>2</sub>ZrO<sub>3</sub> the rate-limiting step is assumed to be the CO<sub>2</sub> diffusion in the solid Li<sub>2</sub>CO<sub>3</sub> shell, whereas in the case of Li/K-doped Li<sub>2</sub>ZrO<sub>3</sub> the rate-limiting step is assumed to be the oxygen ion diffusion in the solid ZrO<sub>2</sub> shell, because the diffusion rate of CO<sub>2</sub> in the molten Li<sub>2</sub>CO<sub>3</sub>/K<sub>2</sub>CO<sub>3</sub> shell is much higher.

From a theoretical point of view we can expect that, during the sorption process and after an initial transient, solid particles composed by an internal core of unreacted Li<sub>2</sub>ZrO<sub>3</sub> and an external shell of ZrO<sub>2</sub> are surrounded by a Li<sub>2</sub>CO<sub>3</sub>/K<sub>2</sub>CO<sub>3</sub> liquid phase. This expectation is also supported by the experimental evidence shown in Figures 11 and 12. From the SEM images shown in Figure 12 it is also clear that the solid particles can be considered approximately spherical in shape. For these reasons, we propose a slightly different model representation to describe the sorption mechanism, which is depicted in Figure 14. Furthermore, we propose a modification to better describe the initial part of the uptake curves, which cannot be accurately captured by the original model based on quasi-steady-state assumption.<sup>6</sup>

According to the model depicted in Figure 14, the overall reaction rate depends on the CO<sub>2</sub> diffusion rate in the Li<sub>2</sub>CO<sub>3</sub>/K<sub>2</sub>CO<sub>3</sub> molten phase and on Li<sup>+</sup>/O<sup>2-</sup> diffusion rates in the ZrO<sub>2</sub> shell. However, since the diffusivity of CO<sub>2</sub> in the liquid phase is much higher than the diffusivity of lithium/oxygen ions in (solid) zirconia, it is reasonable to consider the latter one as the rate-limiting step. Moreover, since the dimension of O<sup>2-</sup> is much

larger than that of Li<sup>+</sup>, the former ion should have much lower diffusivity. For these reasons, we can assume that the overall reaction rate is controlled by the rate of diffusion of O<sup>2-</sup> in the zirconia shell. This diffusion process can be modeled by the following equation:

$$\frac{\partial C_A}{\partial t} = D_A \frac{1}{r^2} \frac{\partial}{\partial r} \left( r^2 \frac{\partial C_A}{\partial r} \right) \quad (5)$$

in which  $C_A$  is the oxygen ion concentration at time  $t$  and generic radius  $r$  inside the ZrO<sub>2</sub> shell;  $D_A$  is the diffusivity of O<sup>2-</sup> in zirconia. In order to simplify the model, we can make use of a quasi-steady-state assumption to obtain the following differential equation:

$$D_A \frac{1}{r^2} \frac{d}{dr} \left( r^2 \frac{dC_A}{dr} \right) = 0 \quad (6a)$$

with associated boundary conditions

$$\begin{aligned} C_A &= C_{A0} & \text{at } r &= L(t) \\ C_A &= C_{A1} & \text{at } r &= R(t) \end{aligned} \quad (6b)$$

in which  $L(t)$  is the radius of the Li<sub>2</sub>ZrO<sub>3</sub> unreacted core and  $R(t)$  is the external radius of the ZrO<sub>2</sub> shell, whereas  $C_{A0}$  and  $C_{A1}$  are the oxygen ion concentrations at inner and outer boundaries of the zirconia shell, respectively (see Figure 14). If we assume that  $R(t)$  does not change significantly, i.e., if we consider the molar density of Li<sub>2</sub>ZrO<sub>3</sub> to be approximately equal to that of ZrO<sub>2</sub>, and denote with  $R_0$  the “constant” value of  $R(t)$ , we can obtain after some manipulations the following equation (more details can be found in ref 6):

$$\frac{dy}{dt} = \alpha \left( \frac{1}{y^2 - y} \right) \quad (7a)$$

with initial condition

$$y(0) = 1 \quad (7b)$$

in which  $y = L(t)/R_0$  and  $\alpha$  is defined as follows:

$$\alpha = \frac{D_A(C_{A0} - C_{A1})}{\rho R_0^2} \quad (8)$$

where  $\rho$  is the molar density of  $\text{ZrO}_2$ . Xiong et al.<sup>6</sup> assume that  $\alpha$  is constant with time and, hence, solve eq 7 analytically. Then, given the value of  $y$  at any time, the relative weight change of the sorbent due to  $\text{CO}_2$  uptake can be evaluated as

$$\hat{z} = \frac{\Delta w}{w_0} = \frac{M_{\text{CO}_2} \rho}{\rho_0} (1 - y^3) \quad (9)$$

in which  $\Delta w$  is the sorbent sample weight change,  $w_0$  is the initial weight of lithium zirconate present in the sample,  $M_{\text{CO}_2}$  is the  $\text{CO}_2$  molecular weight, and  $\rho_0$  is the mass density of  $\text{Li}_2\text{-ZrO}_3$ .

During this work, we experienced that the relative weight change obtained with a constant value of  $\alpha$  does not describe accurately the initial part of the uptake curves, and several reasons can be found for this discrepancy. First of all, during the initial part of the  $\text{CO}_2$  sorption process a proper zirconia shell surrounding the unreacted  $\text{Li}_2\text{ZrO}_3$  is not yet formed. Then, even when this shell is completely formed, neither  $R(t)$  nor the concentration gradient ( $C_{\text{A}0} - C_{\text{A}1}$ ) can be necessarily considered constant. Finally, during the initial sorption process a quasi-steady-state assumption may not be appropriate. Thus, we propose to add transient dynamics for  $\alpha$  as follows:

$$\tau^2 \frac{d^2 \alpha}{dt^2} + 2\tau \frac{d\alpha}{dt} + \alpha = \bar{\alpha} \quad (10a)$$

with initial conditions

$$\alpha(0) = 0, \quad \left. \frac{d\alpha}{dt} \right|_{t=0} = \bar{\alpha} \tau \quad (10b)$$

in which  $\tau$  is a time constant (e.g., expressed in minutes) and  $\bar{\alpha}$  is the asymptotic value of  $\alpha$ . It is important to notice that eq 10 assumes that  $\alpha(t)$  varies from zero to the steady-state value  $\bar{\alpha}$  with second-order dynamics. Furthermore, the lower  $\tau$  the faster  $\alpha(t)$  approaches its steady-state value  $\bar{\alpha}$ . In a preliminary work,<sup>14</sup> we proposed slightly different dynamics for the evolution of  $\alpha$  in the case of Li/K-doped  $\text{Li}_2\text{ZrO}_3$  sorbent prepared with addition of  $\text{Y}_2\text{O}_3$ .

The overall model composed by eqs 7 and 10 is integrated by means of the Matlab ordinary differential equation implicit solver ODE15I, as long as the two parameters  $\tau$  and  $\bar{\alpha}$  are specified, to obtain the time evolution of  $y$  from which the relative weight change of the sorbent can be evaluated by eq 9. The two model parameters  $\tau$  and  $\bar{\alpha}$ , which depend on the operating temperature, are evaluated from a numerical optimization procedure based on experimental data as discussed next.

**4.2. Results and Parameter Optimization.** Given a sequence of  $N$  experimental data of sorbent relative weight changes at different times, we can compute the optimal values of the model parameters  $\tau$  and  $\bar{\alpha}$  by solving the following nonlinear optimization problem:

$$\min_{\tau, \bar{\alpha}} \Phi \quad (11a)$$

subject to

$$\tau_{\min} \leq \tau \leq \tau_{\max} \quad (11b)$$

$$\alpha_{\min} \leq \bar{\alpha} \leq \alpha_{\max} \quad (11c)$$

in which  $\tau_{\min}$ ,  $\tau_{\max}$ ,  $\alpha_{\min}$ , and  $\alpha_{\max}$  are user-defined bounds, and the objective function is defined as

$$\Phi = \sum_{i=1}^N (z_i - \hat{z}_i)^2 \quad (12)$$

where  $z_i$  is the experimental relative weight change measured at time  $t_i$  and  $\hat{z}_i$  is the corresponding relative weight change evaluated from eq 9 with  $y$  computed by model eqs 7 and 10. The optimization problem is numerically solved using the Matlab constrained minimization routine FMINCON.

Since we are interested in modeling the sorption process in a time window where the reaction rate is still high, we restricted our attention to data collected during the first 60 min of  $\text{CO}_2$  uptake. Results for the Li/K-doped  $\text{Li}_2\text{ZrO}_3$  sorbent with a 15% excess of  $\text{Li}_2\text{CO}_3$  at 550 °C are shown in Figure 15, in which it is clear that the proposed model with optimized parameters agrees very well with the experimental data. For comparison, Figure 15 also shows the uptake curve for the original model using a constant value of  $\alpha(t) = \bar{\alpha}$ . It is clear that the initial response of this model is quite different from the experimental curve. Furthermore, even if a lower constant value of  $\alpha$  could be chosen in order to reduce the fitting error, the shape of the model uptake curve would still be inconsistent with the experimental curve. We also evaluated the optimal model parameters for  $\text{CO}_2$  sorption on Li/K-doped  $\text{Li}_2\text{ZrO}_3$  sorbent at 500 and 600 °C. These optimized model parameters are reported in Table 1, from which it appears that the temperature mostly affects the value of  $\bar{\alpha}$ . As expected, the highest value of  $\bar{\alpha}$  is obtained at 550 °C, which is a fairly optimal trade-off temperature between kinetic and thermodynamic factors for the  $\text{CO}_2$  sorption process.

## 5. Conclusions

Carbon dioxide sorption kinetics on different  $\text{Li}_2\text{ZrO}_3$ -based sorbents prepared was investigated in this work.  $\text{Li}_2\text{ZrO}_3$  offers excellent  $\text{CO}_2$  sorption characteristics in terms of large  $\text{CO}_2$  sorption capacity, infinite  $\text{CO}_2/\text{N}_2$  selectivity, and good reversibility. A moderate temperature around 550 °C is desirable for  $\text{CO}_2$  sorption. The  $\text{CO}_2$  sorption rate can increase by the addition of lithium potassium carbonate to  $\text{Li}_2\text{ZrO}_3$  because a molten phase forms at the operating temperature, which increases significantly the  $\text{CO}_2$  diffusion rate. We found that a 15% excess of  $\text{Li}_2\text{CO}_3$  with 0.43  $\text{Li}_2\text{CO}_3$  mole fraction in the carbonate mixture achieves superior results in terms of the sorption rate with respect to other mixtures of carbonates discussed in the literature. Moreover, we found that for this sorbent the addition of  $\text{Y}_2\text{O}_3$  is not necessary and that superior  $\text{CO}_2$  sorption rates are indeed achieved without  $\text{Y}_2\text{O}_3$ . Furthermore, we characterized the regenerability and stability properties of the sorbent, achieving very favorable results. Finally, starting from a double-shell kinetic model described in the literature, we made a number of modifications and proposed a model with two parameters that are found from a nonlinear regression problem based on experimental data. The developed model fits the experimental data very well, and can be readily extended to different operating temperatures by adjusting the two model parameters.

## Acknowledgment

The authors acknowledge the assistance of Piero Narducci for the SEM and XRD analyses.

## Literature Cited

(1) Bredesen, R.; Jordal, K.; Bolland, O. High-temperature membranes in power generation with  $\text{CO}_2$  capture. *Chem. Eng. Process.* **2004**, *43*, 1129.

- (2) Ida, J.; Lin, Y. S. Mechanism of high temperature CO<sub>2</sub> sorption on lithium zirconate. *Environ. Sci. Technol.* **2003**, *37*, 1999.
- (3) Gupta, H.; Fan, L.-S. Carbonation-calcination cycle using high reactivity calcium oxide for carbon dioxide separation from flue gas. *Ind. Eng. Chem. Res.* **2002**, *41*, 4035.
- (4) Hutson, R. D.; Speakman, S. A.; Payzant, A. Structural effects on the high temperature adsorption of CO<sub>2</sub> on a synthetic hydrotalcite. *Chem. Mater.* **2004**, *16*, 4135.
- (5) Reddy, E. P.; Smirniotis, P. G. High-temperature sorbents for CO<sub>2</sub> made of alkali metals doped on CaO supports. *J. Phys. Chem. B* **2004**, *108*, 7794.
- (6) Xiong, R.; Ida, J.; Lin, Y. S. Kinetics of carbon dioxide on potassium-doped lithium zirconate. *Chem. Eng. Sci.* **2003**, *58*, 4377.
- (7) Abanades, J. C. The maximum capture efficiency of CO<sub>2</sub> using a carbonation/calcination cycle of CaO/CaCO<sub>3</sub>. *Chem. Eng. J.* **2002**, *90*, 303.
- (8) Ida, J.; Xiong, R.; Lin, Y. S. Synthesis and sorption properties of pure and modified zirconate. *Sep. Purif. Technol.* **2004**, *36*, 41.
- (9) Brossmann, U.; Knöner, G.; Schaefer, H.-E.; Würschum, R. Oxygen diffusion in nanocrystalline ZrO<sub>2</sub>. *Rev. Adv. Mater. Sci.* **2004**, *6*, 7.
- (10) Zou, Y.; Petric, A. Preparation and properties of yttrium-doped lithium zirconate. *J. Electrochem. Soc.* **1993**, *140*, 1388.
- (11) Knöner, G.; Klaus, R.; Röwer, R.; Södervall, U.; Schaefer, E. Enhanced oxygen diffusivity in interfaces of nanocrystalline ZrO<sub>2</sub>:Y<sub>2</sub>O<sub>3</sub>. *Proc. Natl. Acad. Sci. U.S.A.* **2003**, *100*, 3870.
- (12) Filal, M.; Petot, C.; Mokchah, M.; Chateau, C.; Carpentier, J. L. Ionic conductivity of yttrium-doped zirconia and the "composite effect". *Solid State Ionics* **1995**, *80*, 27.
- (13) Fonseca, F. C.; Muccillo, E. N. S.; Muccillo, R. Analysis of the formation of ZrO<sub>2</sub>:Y<sub>2</sub>O<sub>3</sub> solid solution by the electrochemical impedance spectroscopy technique. *Solid State Ionics* **2002**, *149*, 309.
- (14) Pannocchia, G.; Puccini, M.; Catani, A.; Vitolo, S.; Innocenti, M. High temperature capture of CO<sub>2</sub> on lithium zirconate based sorbents: modelling and experimental studies. In *Proceedings of First Mediterranean Congress Chemical Engineering for Environment*, San Servolo, Venice, Italy; AIDIC: Milano, Italy, 2006.

Received for review December 30, 2006

Revised manuscript received June 28, 2007

Accepted June 29, 2007

IE0616949